



HAL
open science

ImSPOC: A novel compact hyperspectral camera for the monitoring of atmospheric gases

Silvère Gousset, Daniele Picone, Etienne Le Coarer, Juana M. Rodrigo, D. Voisin, Laurence Croizé, Yann Ferrec, Mauro Dalla Mura

► **To cite this version:**

Silvère Gousset, Daniele Picone, Etienne Le Coarer, Juana M. Rodrigo, D. Voisin, et al.. ImSPOC: A novel compact hyperspectral camera for the monitoring of atmospheric gases. IGARSS 2022 - IEEE International Geoscience and Remote Sensing Symposium, Jul 2022, Kuala Lumpur, Malaysia. 10.1109/IGARSS46834.2022.9884258 . hal-04056515

HAL Id: hal-04056515

<https://hal.science/hal-04056515>

Submitted on 3 Apr 2023

HAL is a multi-disciplinary open access archive for the deposit and dissemination of scientific research documents, whether they are published or not. The documents may come from teaching and research institutions in France or abroad, or from public or private research centers.

L'archive ouverte pluridisciplinaire **HAL**, est destinée au dépôt et à la diffusion de documents scientifiques de niveau recherche, publiés ou non, émanant des établissements d'enseignement et de recherche français ou étrangers, des laboratoires publics ou privés.

IMSPOC: A NOVEL COMPACT HYPERSPECTRAL CAMERA FOR THE MONITORING OF ATMOSPHERIC GASES

*S. Gousset*¹, *D. Picone*^{1,2}, *E. Le Coarer*¹, *J. M. Rodrigo*¹, *D. Voisin*³, *L. Croize*⁴, *Y. Ferrec*⁴, *M. Dalla Mura*^{2,5,6}

- (1) Institut of Planetology and Astrophysics of Grenoble, IPAG, Grenoble, France
- (2) Univ. Grenoble Alpes, CNRS, Grenoble INP, GIPSA-lab, 38000 Grenoble, France
- (3) Institut of Environmental Geoscience, IGE, Grenoble, France
- (4) ONERA/DOTA, Chemin de la Hunière, BP 80100, 91123 Palaiseau Cedex, France
- (5) Institut Universitaire de France (IUF), France
- (6) WRHI, School of Computing, Tokyo Institute of Technology, Tokyo, Japan.

ABSTRACT

There is an increasing industrial and scientific demand for large scale monitoring of gas concentration, e.g., to abide with constraints on pollutants for environmental safety. This paper aims to show the potential of the very recent ImSPOC technology for gas monitoring. We present the ImSPOC operating principle, some of the developed prototypes and two illustrative examples in the monitoring of methane and carbon dioxide in controlled environments.

Index Terms— Hyperspectral imaging sensors, Fourier transform imaging spectrometer, Miniaturized sensors, Gas monitoring.

1. INTRODUCTION

Gas monitoring in the atmosphere is a major concern for health and climate, as greenhouse gas emissions and pollutant released from anthropogenic activities are increasing every year. To be able to envision constraint policies on emissions of the main greenhouse gases (e.g., CO₂ and CH₄) and atmospheric pollutants (e.g., NO₂ and O₃), a monitoring at large scale is required, combining both high spatial resolution and frequent temporal coverage. Atmospheric probing both from the ground and remotely sensed from the space are complementary [1]. The former allows for local reference measurements at very high sensitivity and high time frequency, whereas the latter ensures global coverage. Absorption spectroscopy is the mainstream technology of ground and remote sensing instruments to trace gas concentration in the atmosphere through dispersive [2] or Fourier-based spectrometers [3]. Hyperspectral imaging is a key to improve the spatial coverage of space missions, by combining together

imagery of large field of views and spectroscopic measurements. The future Copernicus CO₂ mission [4] will integrate such a device. Nevertheless, the revisit period of the satellite is still too high to ensure improved precision with respect to emission surveys. Payload miniaturization may reduce the cost of a single satellite, allowing to launch a dedicated constellation complementary to the reference missions.

Imaging SPectrometer On Chip (ImSPOC) is a patented concept for a compact snapshot hyperspectral sensor [5] develop for a variety of ground and on-board applications. The aim of this paper is to give an overview on the potential of the ImSPOC technology for gas monitoring. The paper is organized in 3 sections. In Section 2 the concept of ImSPOC is presented. Then, Section 3 describes some integrated prototypes dedicated to gas monitoring. In Section 4, we present some example of experiments we conducted in order to assess gas detection capability of these prototypes. We conclude with a discussion on the open challenges.

2. THE IMSPOC CONCEPT

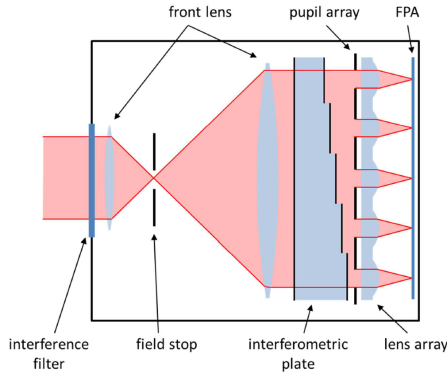
ImSPOC [5] is an innovative concept for a non-conventional compact (i.e., 0.2 to 1 kg) hyperspectral image spectrometer of low-cost and high spectral resolution. As shown in Figure 1 (a), the instrument is composed of a matrix of adjacent interferometers (i.e., Fabry-Pérot etalons) of different thickness, disposed in front of a focal plan array (FPA). Each interferometer is associated with a microlens which focuses onto the FPA an image of the same scene modulated by interferometric fringes depending on the interferometer thickness. In greater detail, the transfer function of an interferometer depends on the wavelength λ and the incident angle θ of the incoming rays. As shown in Figure 1(b) for a fixed angle of incidence θ , after two consecutive inner reflections within the etalon, the interferometer introduces a round trip phase shift $\varphi = 2\pi \frac{\delta}{\lambda}$, where $\delta = 2nL \cos\left(\frac{n}{n_0}\theta\right)$ denotes the optical

This work has been partly supported by a grant from Labex OSUG (ANR10 LABX56), the European Union's H2020 research and innovation program (grant n. 769032) and the ANR FuMultiSPOC (ANR-20-ASTR-0006).

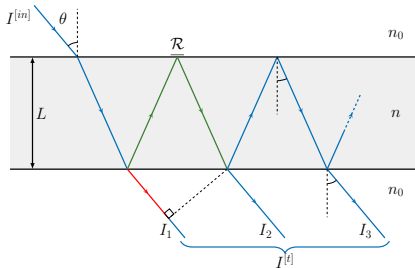
path difference (OPD). Here, L is the thickness of the interferometer, while n and n_0 denote the refraction index within and outside the etalon, respectively. The energy associated to the packet of rays that emerge from the etalon is then ideally focused on a single pixel of the FPA by the associated microlens. The transfer function $A(\lambda, \theta)$ between the transmitted energy and the first emerging ray, for a given interferometer, is given by the following relation, known as Airy's distribution [6]:

$$A(\lambda, \theta) = \left| \sum_{k=0}^{+\infty} \mathcal{R} e^{-jk\varphi} \right| = \frac{1}{(1 - \mathcal{R})^2 + 4\mathcal{R} \sin^2\left(\frac{\varphi}{2}\right)}, \quad (1)$$

where \mathcal{R} denotes the internal reflectivity of the etalon. The Airy's distribution (1) represents a domain transformation of the incident ray from the domain of the wavelengths to that of the OPD, which, in the continuous domain, is commonly known as interferogram. The availability of multiple interferometers allows to sample the interferograms at different OPD; this discretized representation can be inverted to recover the input spectrum, which can then be processed to recover the concentration of the gases to monitor.



(a) ImSPOC optical design.



(b) A Fabry-Pérot interferometer

Fig. 1. The ImSPOC concept. (a) Optical design of a generic ImSPOC device and (b) the operating principle of a single interferometer of thickness L . The OPD can be determined by the difference between the green and the red paths.

3. IMSPOC PROTOTYPES AND APPLICATIONS

The ImSPOC concept can be specialized to address gas monitoring but also a wide range of other applications in remote sensing and planetary science such as the monitoring of vegetation, land/surfaces and solar activity [7]. The characteristics of the components of an ImSPOC device are dependent on the application. For example, the focal plane array used will determine the spatial resolution of the instrument, the spectral filter the spectral sensitivity range and the set of interferometers the frequency filtering and sampling rate. Two spectral domains are currently investigated, leading to different technological components and applications: i) UV-VIS: 300-1000 nm, from the near ultra violet to the cut-off frequency of the silicon based FPA (fully including the visible interval); and ii) SWIR: 800-1700 nm, in the short wave infrared domain.

There are two main modes of operation for the ImSPOC devices: i) the *Hyperspectral mode*, whose target is to capture a finely sampled interferogram in order to reconstruct with high resolution the full spectrum in the sensitivity range of the instrument making this a general purpose device; and ii) the *Specialized mode*, where the sampling of the interferogram is optimized with respect to a target of interest in the Fourier domain. This mode of operation is application-oriented and allows, for instance to correlate some CO_2 and CH_4 absorption spectral patterns in dedicated ImSPOC cameras [8], as presented in the experiments of the next section. Figure 2 presents some gas dedicated ImSPOC prototypes, and their associated characteristics.

4. GAS MONITORING USING IMSPOC

We present in this section some preliminary experimental results to illustrate the gas detection capability of the ImSPOC prototypes.

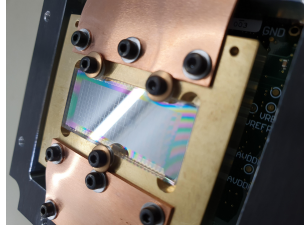
A first experiment aims at measuring the signal quality of a methane-dedicated ImSPOC-based camera in a controlled in-lab acquisition. A wide spectrum source is focused within a 10 cm long gas cell before entering into an integrated sphere. The camera is oriented towards the output port of the sphere, so that the whole field of view (FoV) is illuminated homogeneously. The methane flow in the gas cell is controlled; as the cell is not hermetically sealed, the pressure in the cell is around 1 atm for the whole duration of the experiment. At the beginning, the cell is filled with air then the methane starts flowing and stops once the cell gets fully saturated. The acquisitions after the methane flow has stopped allow to study the release of the methane from the cell. Figure 3(a) shows a comparison between the raw acquisitions before and after the methane injection: the image initially does not show any pattern (left), while interference rings clearly appear when the methane is present (right). Figure 3(b) compares the histogram of the intensity of these two images as a function of the phase term (modulo 2π) expressed



(a) CO₂ and CH₄ dedicated ImSPOC cameras.



(b) SWIR ImSPOC cam.



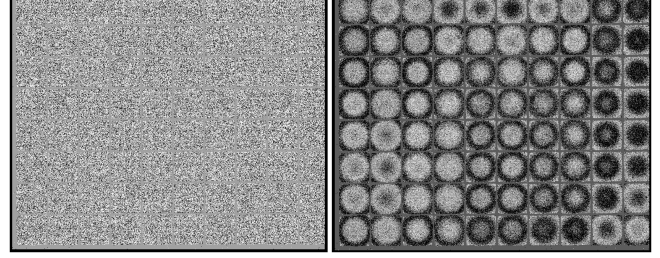
(c) Visible ImSPOC cam.

Fig. 2. Some ImSPOC prototypes dedicated to gas monitoring. (a) CO₂ and CH₄ dedicated ImSPOC SWIR cameras, designed for airborne detection of gas plumes, 64×64 pixels in the field of view (15°), 2 kg each. (b) SWIR ImSPOC hyperspectral camera designed for UAV: 40 spectral bands in range 1200-1700 nm, 64×64 pixels fov (15°), < 0.5 kg. (c) Visible ImSPOC hyperspectral camera (without front baffle) for sky monitoring: ~100 spectral bands in 380–1000 nm, 96×96 fov (15°), 0.5 kg.

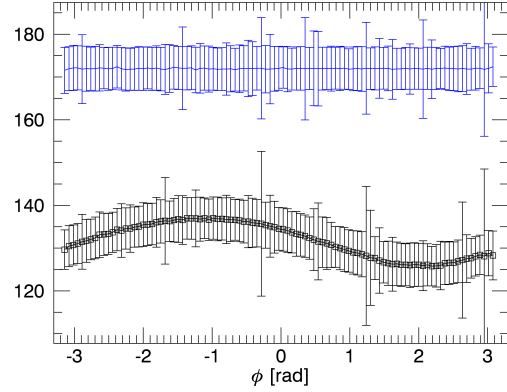
in Eq. 1. When the cell is filled by air (blue curve) the signal follows a Poisson distribution showing a uniform dependency with the phase. When methane is present (black curve), an almost-sinusoidal fringe appears as expected and formalized by Eq. 1. We then analyse the temporal evolution of the acquisitions while the cell fills up with methane. Figure 4 shows the mean signal level for each acquired frame with respect to the ratio between the modulation amplitude and the mean level of the interferogram (i.e. fringe visibility). As expected, the two parameters have an inverse trend: when the methane concentration increases, light is absorbed and the mean of the signal decreases with interference patterns of increasingly higher contrast (increased visibility) appearing. This first experiment shows that the designed camera is responsive to the methane spectroscopic signature, showing an encouraging capability to detect atmospheric methane.

In the second experiment, we study the evolution of the integrated slant column of CO₂ during a day using a CO₂-specialized ImSPOC camera pointing at the Sun and taking acquisitions every ten seconds.

Figure 5 presents the recorded signal visibility with respect to the time of the acquisition during the day. For each acquisition, we plot on the Y-axis the visibility histogram for all the pixels of the image. The white curve stands for aver-



(a)



(b)

Fig. 3. Laboratory experiment of methane detection in a gas cell with a specialized ImSPOC-based camera. (a) Acquisition frame before (left) and after (right) the introduction of methane. (b) Signal histogram as a function of the interferometric state (phase). In blue, when filled with air, and in black, with methane saturated at atmospheric pressure.

aged visibility over all the pixels. Several time sequences of acquisitions are missing, and a sensor malfunction occurred in the segment before 15:00. As a consequence data are not continuous.

By using formula of the airmass factor (AMF) described in [9], we are able to estimate that the airmass is approximately multiplied by a factor 1.4 from 14:00 UTC ($z = 62.5^\circ$, $AMF \approx 2.16$) to 15:00 ($z = 70.79^\circ$, $AMF \approx 3.01$). By analyzing the obtained results, the visibility measured from 14:00 to 15:00 increases from about 0.024 to 0.030, leading to a factor of $0.030/0.024 = 1.25$ which is quite close to the estimated AMF multiplication value of 1.4. The relative error of 10% is related to the airmass approximation we used while z becomes close to 80° . We must integrate some additional atmospheric features as refraction and layered species distribution, in a more complex model. This simple proof of concept shows that the ImSPOC technology has a potential for the characterization of the atmospheric absorption, representing a first step towards an operational gas sensor for space applications.

In addition to these two preliminary experiments, some results about CO₂ and CH₄ monitoring from an aircraft us-

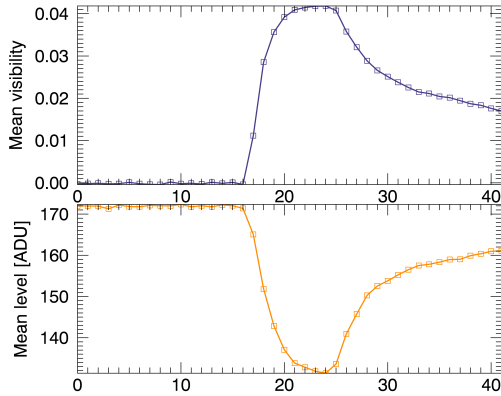


Fig. 4. Temporal evolution of the mean signal and the mean interferometric visibility. Frame numbers are reported on the horizontal axis, one tick interval corresponds to 150 ms. The cell is filled with air until frame-16. A constant flow of methane then fills the cell until frame-24 when it stops and pressure decreases.

ing the devices we presented in this paper have been reported in [10] for a smallsat constellation feasibility study. Furthermore, a non-specialized ImSPOC prototype operating in the visible domain has been considered for NO_2 detection in [11].

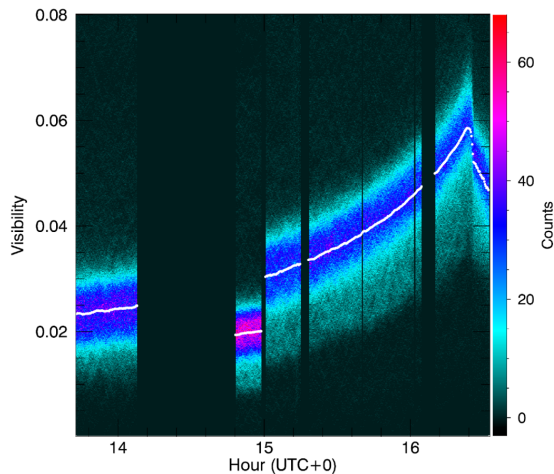


Fig. 5. Temporal histogram of interference visibility during a solar view with a CO_2 -specialized prototypes.

5. DISCUSSION AND CONCLUSION

This work presented an overview of the ImSPOC technology. The preliminary results obtained in two controlled experiments illustrate the potential of the ImSPOC concept for the monitoring of atmospheric gases.

While this recent technology shows an enormous potential thanks to its high spectral resolution, compactness and

low-cost, there are several open challenges. The most relevant problems lie in the signal processing, as the acquisitions are taken in a domain different to the one that is desired for the final applications, hence requiring a carefully designed pipeline of algorithms of data processing to recover the desired information. Such pipeline typically includes, image coregistration, characterization of the transfer function and inversion of the interferograms [12]. Moreover, in comparison with the controlled scenarios presented here, further complications are expected when the FoV is not illuminated homogeneously (i.e., when considering real scenes with complex structures) and when the interferometric signal is dominated by the scene dynamics, which can be typically two orders of magnitude greater than the target absorption patterns.

6. REFERENCES

- [1] P. Ciaia et al., “Atmospheric inversions for estimating CO_2 fluxes: methods and perspectives,” in *Greenhouse Gas Inventories*, pp. 69–92. Springer, 2010.
- [2] F. Pasternak et al., “The microcarb instrument,” in *ICSO 2016*. 2017, vol. 10562, p. 105621P, International Society for Optics and Photonics.
- [3] T. Hamazaki et al., “Fourier transform spectrometer for Greenhouse Gases Observing Satellite (GOSAT),” in *SPIE*. Jan. 2005, vol. 5659, pp. 73–80, SPIE.
- [4] J-L. Bézy et al., “The European Copernicus Anthropogenic CO_2 Monitoring Mission,” in *IGARSS 2019*, July 2019, pp. 8400–8403, ISSN: 2153-7003.
- [5] N. Guerineau et al., “U.S. Patent No. 10,677,650,” 2020.
- [6] I. Nur et al., “Fabry-pérot resonator: spectral line shapes, generic and related airy distributions, linewidths, finesses, and performance at low or frequency-dependent reflectivity,” *Optics Express*, vol. 24, no. 15, pp. 16366, July 2016.
- [7] E. Le Coarer et al., “Optimization of a compact static interferometer based on ImSPOC technology for a wide field polar lights monitoring,” in *ICSO 2020*. June 2021, vol. 11852, pp. 595–608, SPIE.
- [8] S. Gousset et al., “NanoCarb hyperspectral sensor: on performance optimization and analysis for greenhouse gas monitoring from a constellation of small satellites,” *CEAS Space Journal*, Sept. 2019.
- [9] K. A. Pickering, “The southern limits of the Ancient Star Catalog and the Commentary of Hipparchos,” *DIO*, vol. 12, pp. 3–27, 2002.
- [10] S. Gousset et al., “NanoCarb spaceborne miniaturized GHG sensor: first experimental results,” in *ICSO 2020*. June 2021, vol. 11852, pp. 1106–1127, SPIE.
- [11] Y. Bourdin et al., “ NO_2 vertical column density estimation from interferograms captured by a snapshot interferometric imaging spectrometer,” Tech. Rep. EGU22-2926, Copernicus Meetings, 2022, EGU22.
- [12] D. Picone, *Model based signal processing techniques for non-conventional optical imaging systems*, Ph.D. thesis, Université Grenoble Alpes, EEATS, 2021.